

# A maximum spreading speed for magnetopause reconnection

B. M. Walsh<sup>1</sup>, D.T. Welling<sup>2</sup>, Y. Zou<sup>3,4</sup>, Y. Nishimura<sup>3</sup>

<sup>1</sup>Center for Space Physics, Department of Mechanical Engineering, Boston University, USA

<sup>2</sup>AOSS, University of Michigan, Ann Arbor, Michigan, USA

<sup>3</sup>Center for Space Physics, Boston University, USA

<sup>4</sup>Cooperative Programs for the Advancement of Earth System Science, University Corporation for Atmospheric Research,  
Boulder, Colorado, USA

## Key Points:

- Solar wind fronts can spread across the magnetopause at over 850 km/s
- The speed of convecting solar wind structures contacting along the magnetopause does not limit the spreading of magnetic reconnection under typical conditions

This is the author manuscript accepted for publication and has undergone full peer review but has not been through the copyediting, typesetting, pagination and proofreading process, which may lead to differences between this version and the [Version of Record](#). Please cite this article as doi: [10.1029/2018GL078230](https://doi.org/10.1029/2018GL078230)

---

Corresponding author: Brian Walsh, [bwalsh@bu.edu](mailto:bwalsh@bu.edu)

This article is protected by copyright. All rights reserved.

## Abstract

Past observations and numerical modeling find magnetic reconnection to initiate at a localized region and then spread along a current sheet. The rate of spreading has been proposed to be controlled by a number of mechanisms based on the properties within the boundary. At the Earth's magnetopause the spreading speed is also limited by the speed at which a shocked solar wind front can move along the magnetopause boundary. The speed at which a purely north to south rotational discontinuity propagates through the magnetosheath and contacts the magnetopause is measured here using the BATSUS global magnetohydrodynamics model. The propagation speed along the magnetopause is fastest near the nose of the magnetopause and decreases with distance from the subsolar point. The average propagation speed along the dayside magnetopause is 847 km/s. This is significantly larger than observed rates of reconnection spreading at the magnetopause of 30-40 km/s indicating that, for the observed conditions, the speed of front propagation along the magnetopause does not limit or control the spreading rate of reconnection.

## 1 Introduction

At the start of magnetic reconnection's life cycle is birth and then growth. Birth or initiation is generally thought to occur in a current sheet at a small, localized position and then expand out of the reconnecting plane [Milan *et al.*, 2000; Shay *et al.*, 2003]. With application to the Earth's magnetopause, this growth or spreading in the out-of-plane direction occurs across the boundary in local time. Figure 1 presents a diagram of this growth and geometry.

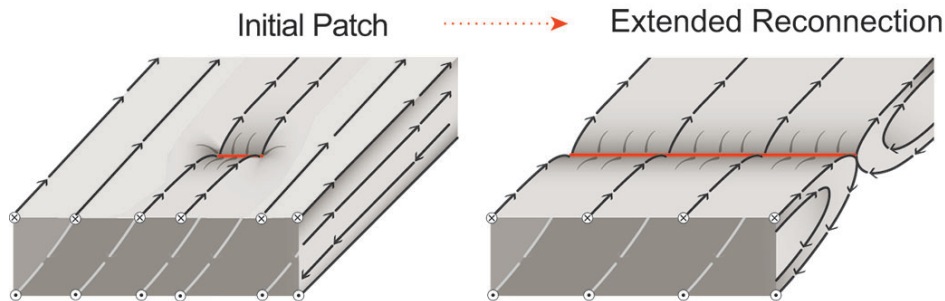


**Figure 1.** Schematic diagram of reconnection spreading. Initiation occurs in a spatially localized region (left) and spreads into an extended line (right). The region of reconnection is shown in red.

The rate of spreading has significant implications in a number of systems. At a planetary magnetosphere this spreading rate, and subsequently the length of the magnetopause x-line, controls how much energy is coupled from the solar wind [Milan *et al.*, 2012]. The speed of spreading is relevant for component [Crooker, 1979; Luhmann *et al.*, 1984] and antiparallel [Gonzalez and Mozer, 1974] magnetopause reconnection as well as other local-physics based models predicting the location of reconnection [Swisdak and Drake, 2007; Hesse *et al.*, 2013]. This spreading process is also monitored in the solar environment through the elongation of flare ribbons [Tripathi *et al.*, 2006; Li and Zhang, 2009; Qiu *et al.*, 2017], as well as in lab plasmas [Katz *et al.*, 2010; Dorfman *et al.*, 2014].

Several models have been proposed to describe reconnection spreading. At the core of the problem, information needs to be transported away from where reconnection is initiated. One model suggests the expansion is driven by a current out of the reconnecting plane [Huba and Rudakov, 2002; Shay *et al.*, 2003; Lapenta *et al.*, 2006; Neeraj *et al.*,

2013]. A second model proposes that reconnection spreading results from Alfvén waves and would occur at a velocity equal to the out of plane Alfvén speed [Katz *et al.*, 2010]. A third possibility is a combination of the previous two. Here both mechanisms are capable of driving expansion, and the actual speed is the maximum of the two [Shepherd and Cassak, 2012].

These theories and supporting numerical simulations have been based on models with flat current sheets and static boundary conditions. By contrast, a planetary magnetopause is a curved surface and the boundary conditions are temporally variable. A front or discontinuity in the solar wind will pass through the bow shock, contact the nose of the magnetopause, and then be swept downtail where it contacts the tail magnetopause at later times. If this solar wind discontinuity were a rotation of the magnetic field from purely northward to purely southward, it would strike the subsolar magnetopause first, likely initiating reconnection near local noon, and then contact other places as the front convects tailward in the magnetosheath. The speed of this front’s motion through the magnetosheath provides an additional constraint to the spreading speed of magnetopause reconnection. No matter how fast the current carriers or Alfvén waves may want to propagate, reconnection can not spread beyond the extent of the high shear angle magnetopause current sheet. The speed of the front along the boundary is therefore the maximum speed of expansion. This paper measures the propagation speed of a rotational discontinuity along the magnetopause in a global MHD model and compares this value with experimentally measured spreading speeds from previous work.

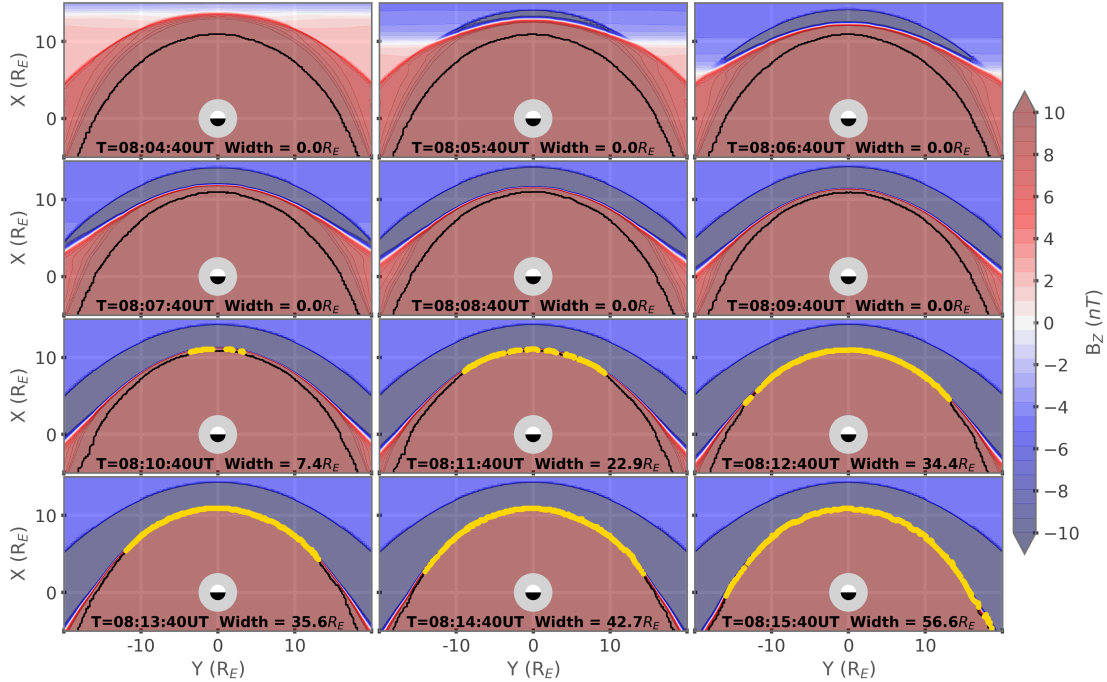
## 2 Numerical Experiment

The Block-Adaptive-Tree Solar Wind Roe-Type Upwind Scheme (BATSRUS) model [Powell *et al.*, 1999; Tóth *et al.*, 2005, 2012] was run to monitor the propagation of a solar wind front. Grid set up follows that of Welling and Liemohn [2014] with the resolution improved to  $1/8 R_E$  within a block spanning  $\pm 16 R_E$  in the GSM Y direction,  $\pm 8 R_E$  in the GSM Z direction, and  $-4$  to  $+12 R_E$  in the GSM X direction. A total of 10.65 million computational cells were used. Solar wind flow conditions were held constant with an Earthward flow speed of 400 km/s, a hydrogen number density of  $5 \text{ cm}^{-3}$ , and a temperature of  $1.2 \times 10^5$  K. To properly initialize the magnetosphere, the IMF was first southward oriented for two hours of simulation time (IMF  $B_Z = -2$  nT), then rotated northward for another six hours ( $B_Z = +2$  nT), allowing the system to achieve pseudo steady-state.

To provide a direct comparison with spreading observations from Zou *et al.* [2018], the IMF was rotated southward (IMF  $B_Z = -5$  nT) at 8 hours into the simulation. As time progressed, the rotational front moved Earthward through the magnetosheath and draped along the magnetopause.  $B_Z$  contours in the GSM equatorial plane as a function of time are presented in Figure 2. Red contours correspond to regions of northward magnetic field, blue contours show regions of southward magnetic field.

To quantify when and where the front contacted the magnetopause, profiles of  $B_Z$  were drawn radially outward from the Earth. If a  $B_Z < 0$  value was measured within  $1/4 R_E$  of the open/closed magnetic field boundary along the radial profile, the front was defined to be “contacting” the magnetopause at that location. Since the resolution of the MHD simulation was  $1/8 R_E$  at the magnetopause, the range spanned 2 grid points. The boundary between open and closed magnetic field topology was identified through magnetic field line tracing.

The front first contacted the magnetopause near local noon at 8:10:40 in the simulation time. As time continued, the local time of the contacted region along the magnetopause grew. Measurements of the spreading are presented in Figure 3. The top frame shows the limits of the contact region in the GSM Y direction; the middle frame shows the integrated length of the contact region along the magnetopause. Although the local



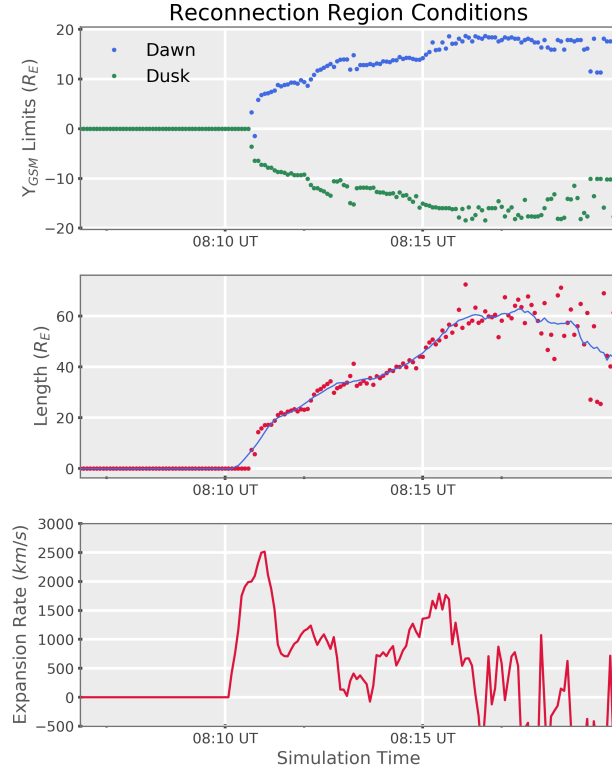
86 **Figure 2.** Slices of the  $B_z$  component of the magnetic field with 1 minute time cadence in the XZ GSM  
 87 plane. The yellow dots indicate a value of  $-B_z$  is contacting the magnetopause at that local time.

100 time extent of the front’s contact region expanded in local time, the rate of expansion was  
 101 not constant. The bottom panel of Figure 3 presents the expansion rate as a function of  
 102 time. The largest expansion rate of 2503 km/s occurred during the 1 minute period just  
 103 as the front contacted the subsolar magnetopause. Although the flow speed in the magne-  
 104 tosheath is low near the subsolar region [Walsh *et al.*, 2012; Dimmock and Nykyri, 2013],  
 105 there is a relatively large angle between the boundary plane and the sun-Earth line. This  
 106 means a small motion of the front in the GSM X direction will translate to a large expansion  
 107 in GSM Y, and thus local time.

108 After the brief period ( $\sim 1$  minute) with rapid expansion along the boundary, the ex-  
 109 pansion rate was fairly steady for  $\sim 7$  minutes at 825 km/s. During this period the  $-B_z$   
 110 front spread along the boundary to contact a region extending close to  $60 R_E$  in local  
 111 time. At this point ( $\sim 8:17$  in the simulation) the measured length became variable around  
 112 a length of  $60 R_E$  and did not expand further. At local times near the terminator the magne-  
 113 topause boundary became turbulent, and inspection of the bulk flow and magnetic topol-  
 114 ogy presents evidence for boundary waves and flux transfer events. Additionally, the magne-  
 115 topause boundary increases in thickness with distance from local noon. As the bound-  
 116 ary becomes thicker it will not be detected as a “contacted” boundary with the used met-  
 117 ric. These conditions may limit the ability to measure expansion beyond the terminator,  
 118 however since the primary objective is the study is to measure expansion speeds along the  
 119 dayside magnetopause they are not problematic.

125 **3 Discussion**

126 As the front moved through the bow shock and into the magnetosheath it bent around  
 127 the obstacle of the magnetosphere. Similar results have been found experimentally through  
 128 studies monitoring how an interplanetary shock passed through the magnetosheath [Keika



120 **Figure 3.** Front spreading along the magnetopause boundary. The top panel presents the GSM y position  
 121 of the extension of the front in the dawn (blue) and dusk (green) direction. Each point corresponds to a single  
 122 5 s MHD step. The middle panel is the length integrated along the magnetopause from the dawn extent to the  
 123 dusk extent. The blue trace is a running average. The bottom panel is the rate of expansion of the front along  
 124 the magnetopause.

129 *et al.*, 2009]. Although many fronts that contact the magnetopause are close to perpendicular  
 130 to the Earth-Sun line, they can also be inclined or have different orientations. Studies  
 131 modeling the dynamics of inclined shocks striking the magnetopause have shown as  
 132 a structure becomes more inclined, the position at which it first strikes the magnetopause  
 133 moves away from the subsolar point [Samsonov, 2011; Oliveira and Raeder, 2014; Sam-  
 134 sonov *et al.*, 2015]. The geometry of where a front first strikes the magnetopause will in  
 135 turn impact the spreading speed. Since the ionospheric signatures of reconnection in the  
 136 event being simulated here commence near local noon, it is a reasonable assumption the  
 137 front was close to perpendicular to the Earth-Sun line.

### 138 3.1 Front Propagation Speeds and Reconnection Spreading

139 At a planetary magnetosphere embedded within a flowing solar wind, IMF structures  
 140 will strike the nose of the magnetopause and then propagate tailward along the bound-  
 141 ary. This speed of propagation will limit the maximum spreading speed of magnetic re-  
 142 connection in the system. In the case of a discontinuity in the solar wind with a rotation  
 143 from positive to negative  $B_z$ , reconnection is anticipated to be initialized at the subso-  
 144 lar point of the magnetopause when the discontinuity contacts the boundary. No matter  
 145 how quickly reconnection may want to spread, the process is limited by the propagation  
 146 speed of the magnetosheath magnetic field discontinuity along the magnetopause. For  
 147 some boundary conditions, this process may not limit reconnection spreading. In a current

**Table 1.** Spreading speeds at the magnetopause. Values marked with † are from *Zou et al.* [2018].

| Type                    |                          | Value     |
|-------------------------|--------------------------|-----------|
| Theory - Alfvén speed   | $v_{Alfven}^{\dagger}$   | 71.6 km/s |
| Theory - Current speed  | $v_J^{\dagger}$          | 89.8 km/s |
| Experimental ionosphere | $v_{Observed}^{\dagger}$ | 39.9 km/s |
| Numerical front speed   | $v_{MHDFront}$           | 847 km/s  |

sheet with very little guide field and a small current, one may not anticipate reconnection to spread quickly based on current theory. By contrast, for a boundary with a large guide field (large out of plane Alfvén speed) or a large current velocity, reconnection may be limited by the magnetosheath front speed.

### 3.2 Comparison with Past Measurements

Using projected measurements of ionospheric flows, *Zou et al.* [2018] was able to create estimates for magnetopause reconnection spreading rates. In the two events analyzed, the measured spreading rates were less than those predicted by theory. Table 1 presents the spreading speeds obtained by *Zou et al.* [2018] from 23 May 2014 as well as the front velocity from the current study. As noted previously, theory predicts that the spreading speed will be the maximum velocity of either the out of plane Alfvén speed ( $v_A$ ) or the current carrier speed ( $v_J$ ) [*Shepherd and Cassak, 2012*]. The out of plane Alfvén speed is described as  $v_A = \frac{B_m}{\sqrt{\mu_0 \rho}}$  where  $B_m$  is the out of plane magnetic field or guide field,  $\mu_0$  is the permeability of free space, and  $\rho$  is the mass density. The current velocity is  $v_J = \frac{J}{ne}$  where  $J$  is the current density,  $n$  is the number density, and  $e$  is the charge of an electron. The upstream solar wind conditions in the current study were chosen to match those from the 23 May 2014 event. The expansion speed of the front along the boundary found through MHD is more than an order of magnitude larger than the measured and theoretical values of the reconnection spreading speed. This indicates the front expansion speed does not play a significant role in controlling or limiting the spreading speed.

### 3.3 Reconnection Rotation

A possible alternative model to spreading reconnection is that reconnection is always active somewhere at the magnetopause. In this model, rather than starting as a small patch and growing, an extended x-line is omni-present and will just shift its position in response to IMF rotations or changes in the solar wind. Although the community has long studied the steady-state location of dayside magnetopause reconnection [*Pu et al., 2007; Trenchi et al., 2008*], very little observational work has been conducted monitoring the dynamic motion (or death) of an x-line. One requirement of the “rotating reconnection line” model is that structures or regions of active reconnection along the magnetopause boundary can be relatively steady and will sometimes move sunward during rotations. Hybrid and kinetic numerical modeling results are not consistent with this picture. These models present a dynamic system where reconnection commonly turns on, off, and moves tailward, even for steady solar wind conditions [*Sibeck and Omidi, 2012; Hoilijoki et al., 2017*]. In these models it is uncommon for reconnecting structures to move in the sunward direction.

Observations have also reported magnetopause reconnection to be both limited [*Ok-savik et al., 2004; Milan et al., 2016; Walsh et al., 2017*] as well as extended in local time [*Phan et al., 2000; Dunlop et al., 2011*]. Varying spatial extents along the boundary is

187 consistent with a model where reconnection can be transient and growing with time. It is  
188 not strictly consistent with an omni-present reconnection line. Similar results are found in  
189 the ionosphere. Rather than an omnipresent aurora or region of convection that may result  
190 from omnipresent magnetopause reconnection, ionospheric measurements find signatures  
191 that fade/die and reform corresponding to different regions of reconnection turning off and  
192 on at the magnetopause [Sandholt and Farrugia, 2002; Zou et al., 2018].

### 193 3.4 Observational Signatures

194 If the rotational front indeed passes by the magnetosphere faster than reconnection  
195 can spread in local time from the point of first contact, there are several features  
196 that should be observable with spacecraft measurements. Depending on how reconnection  
197 manifests, an observer should either find discontinuous patches of reconnection, or  
198 time periods where reconnection is observed near local noon but not at other local times.  
199 The patchy reconnection scenario would occur once a front of  $-B_z$  in the magnetosheath  
200 has draped itself over a range of local times at the magnetopause, but the initial patch of  
201 reconnection near local noon has not had time to spread. This would leave large spatial  
202 areas with significant magnetic shear at the magnetopause which could reconnect locally  
203 and start spreading themselves. This is similar to the scenario found in simulations of the  
204 magnetotail plasmashet where many spatially localized patches form initially and coalesce  
205 into a larger continuous x-line [Shay et al., 2003].

206 Alternatively, a scenario may exist where reconnection can only be initiated at the  
207 nose of the magnetopause or the place of first contact. This may be due to the thickness  
208 of the boundary layer or the presence of stabilizing flows in the magnetosheath off local  
209 noon. In this scenario, once again, one should be able to observe active reconnection at  
210 or near local noon, but regions away from noon with large magnetic sheath and no active  
211 reconnection.

## 212 4 Conclusions

213 A global BATSRUS MHD simulation was used to monitor the rate at which a  $+B_z$   
214 to  $-B_z$  discontinuity passed through the magnetosheath and draped along the magnetopause.  
215 The expansion speed of a front along the magnetopause boundary is important as it serves  
216 as a limit for the maximum spreading speed of magnetopause reconnection. The  $-B_z$  front  
217 contacted the nose of the magnetopause and expanded past the terminator in 7 minutes,  
218 corresponding to an average expansion speed in local time along the boundary of 847  
219 km/s. The simulation was designed with similar solar wind conditions to a previous ob-  
220 servational experiment which found magnetopause reconnection to expand at 30-40km/s.  
221 Since the front expansion is much larger than the observed spreading rates it is concluded  
222 that the expansion rate of a solar wind front along the magnetopause does not limit the  
223 spreading rate for the current event and others with similar solar wind conditions.

### 224 Acknowledgments

225 Support was given by the NASA grants NNX16AJ73G and NNX16AD91G. NSF support  
226 was provided by grant AGS-1502436. Analysis of the MHD results was performed using  
227 the Spacepy software library [Morley et al., 2011]. The authors would like to thank R.  
228 Lopez for useful discussions. MHD simulation files generated and used as part of this  
229 study are available online through the following,

230 [https://deepblue.lib.umich.edu/data/concern/generic\\_works/sj1392745?locale =](https://deepblue.lib.umich.edu/data/concern/generic_works/sj1392745?locale=en)  
231 [en.](https://deepblue.lib.umich.edu/data/concern/generic_works/sj1392745?locale=en)

## References

- 233 Crooker, N. U. (1979), Dayside merging and cusp geometry, *J. Geophys. Res.*, *84*(A3),  
 234 951-959, doi: 10.1029/JA084iA03p00951.
- 235 Dimmock, A. P., and K. Nykyri (2013), The statistical mapping of magnetosheath  
 236 plasma properties based on THEMIS measurements in the magnetosheath inter-  
 237 planetary medium reference frame, *J. Geophys. Res. Space Physics*, *118*, 4963-4976,  
 238 doi:10.1002/jgra.50465.
- 239 Dorfman S., Ji, H., Yamada, M., Yoo, J., Lawrence, E., Myers, C., and Tharp, T. (2014).  
 240 Experimental observation of 3-D, impulsive reconnection events in a laboratory plasma.  
 241 *Physics of Plasmas* *21*(1), 012109. doi:10.1063/1.4862039.
- 242 Dunlop, M. W., et al. (2011), Magnetopause reconnection across wide local time, *Ann.*  
 243 *Geophys.*, *29*, 1683.
- 244 Gonzalez, W. D., and F. S. Mozer (1974), A quantitative model for the potential result-  
 245 ing from reconnection with an arbitrary interplanetary magnetic field, *J. Geophys. Res.*,  
 246 *79*(28), 4186-4194, doi: 10.1029/JA079i028p04186.
- 247 Hesse, M., N. Aunai, S. Zenitani, M. Kuznetsova, and J. Birn (2013), Aspects of colli-  
 248 sionless magnetic reconnection in asymmetric systems, *Phys. Plasmas*, *20*(6), 061210,  
 249 doi:10.1063/1.4811467.
- 250 Hoilijoki, S., U. Ganse, Y. Pfau-Kempf, P. A. Cassak, B. M. Walsh, H. Hietala, S. von  
 251 Alfthan, and M. Palmroth (2017), Reconnection rates and X line motion at the mag-  
 252 netopause: Global 2D-3V hybrid-Vlasov simulation results, *J. Geophys. Res. Space*  
 253 *Physics*, *122*, doi:10.1002/2016JA023709.
- 254 Huba, J. D., and L. I. Rudakov (2002), Three-dimensional Hall magnetic reconnection,  
 255 *Phys. Plasmas*, *9*, 4435.
- 256 Katz, N., Egedal, J., Fox, W., Le, A., Bonde, J., and Vrublevskis, A. (2010), Labora-  
 257 tory observation of localized onset of magnetic reconnection. *Physical Review Letters*,  
 258 *104*(25), 255004. doi:10.1103/PhysRevLett.104.255004.
- 259 Keika, K., et al. (2009), Deformation and evolution of solar wind discontinuities  
 260 through their interactions with the Earth's bow shock, *J. Geophys. Res.*, *114*, A00C26,  
 261 doi:10.1029/2008JA013481.
- 262 Lapenta, G., D. Krauss-Varban, H. Karimabadi, J. D. Huba, L. I. Rudakov, and P. Ricci  
 263 (2006), Kinetic simulations of X-line expansion in 3D reconnection, *Geophys. Res. Lett.*,  
 264 *33*, L10102, doi:10.1029/2005GL025124.
- 265 Li, L., and J. Zhang (2009), On the Brightening Propagation of Post-Flare Loops Ob-  
 266 served by TRACE, *ApJ*, *690*, 1, doi:10.1088/0004-637X/690/1/347.
- 267 Luhmann, J. G., R. J. Walker, C. T. Russell, N. U. Crooker, J. R. Spreiter, and S. S. Sta-  
 268 hara (1984), Patterns of potential magnetic field merging sites on the dayside magne-  
 269 topause, *J. Geophys. Res.*, *89*(A3), 1739-1742, doi: 10.1029/JA089iA03p01739.
- 270 Milan, S. E., M. Lester, S. W. H. Cowley, and M. Brittnacher (2000), Convection and au-  
 271 roral response to a southward turning of the IMF: Polar UVI, CUTLASS, and IMAGE  
 272 signatures of transient magnetic flux transfer at the magnetopause, *J. Geophys. Res.*,  
 273 *105*(A7), doi:10.1029/2000JA900022.
- 274 Milan, S. E., J. S. Gosling, and B. Hubert (2012), Relationship between interplanetary  
 275 parameters and the magnetopause reconnection rate quantified from observations of the  
 276 expanding polar cap, *J. Geophys. Res.*, *117*, A03226, doi:10.1029/2011JA017082.
- 277 Milan, S. E., S. M. Imber, J. A. Carter, M.-T. Walach, and B. Hubert (2016), What con-  
 278 trols the local time extent of flux transfer events?, *J. Geophys. Res. Space Physics*, *121*,  
 279 doi:10.1002/2015JA022012.
- 280 Morley, S., Welling, D., Koller, J., Larsen, B. A., Henderson, M. G., and Niehof, J.  
 281 (2011). SpacePy - a python-based library of tools for the space sciences. Proceeding  
 282 of the 9th Python in Science Conference, Austin, TX, 39 - 45.
- 283 Neeraj J., J. Buchner, S. Dorfman, H. Ji, and A. S. Sharma (2013), Current disruption and  
 284 its spreading in collisionless magnetic reconnection, *Physics of Plasmas*, *20*, 112101,



285  
286  
287  
288  
289  
290  
291  
292  
293  
294  
295  
296  
297  
298  
299  
300  
301  
302  
303  
304  
305  
306  
307  
308  
309  
310  
311  
312  
313  
314  
315  
316  
317  
318  
319  
320  
321  
322  
323  
324  
325  
326  
327  
328  
329  
330  
331  
332  
333  
334  
335  
336  
337  
338

doi:10.1063/1.4827828.

Oksavik, K., J. Moen, and H. C. Carlson (2004), High-resolution observations of the small-scale flow pattern associated with a poleward moving auroral form in the cusp, *Geophys. Res. Lett.*, 31, doi:10.1029/2004GL019838, 2004.

Oliveira, D. M., and J. Raeder (2014), Impact angle control of interplanetary shock geoeffectiveness, *J. Geophys. Res. Space Physics*, 119, 8188-8201, doi:10.1002/2014JA020275.

Phan, T. D., L.M Kistler, B. Klecker, G. Haerendel, G., Paschmann, B.U. Ö. Sonnerup, et al. (2000). Extended magnetic reconnection at the Earth's magnetopause from detection of bi-directional jets. *Nature*, 404(6780), 848-850. doi:10.1038/35009050.

Powell, K. G., P. L. Roe, T. J. Linde, T. I. Gombosi, and D. L. De Zeeuw (1999), A solution-adaptive upwind scheme for ideal magnetohydrodynamics, *J. Comput. Phys.*, 154, 284.

Pu, Z. Y., et al. (2007), Global view of dayside magnetic reconnection with the dusk-dawn IMF orientation: A statistical study for Double Star and Cluster data, *Geophys. Res. Lett.*, 34, L20101, doi:10.1029/2007GL030336.

Qiu, J., D.W. Longcope, P.A. Cassak, and E.R. Priest (2017), Elongation of Flare Ribbons, *Astrophysical Journal*, 838, 17, doi:10.3847/1538-4357/aa6341.

Samsonov, A. A. (2011), Propagation of inclined interplanetary shock through the magnetosheath, *J. Atmos. Sol. Terr. Phys.*, 73, 30-39, doi:10.1016/j.jastp.2009.10.014.

Samsonov, A. A., V. A. Sergeev, M. M. Kuznetsova, and D. G. Sibeck (2015), Asymmetric magnetospheric compressions and expansions in response to impact of inclined interplanetary shock, *Geophys. Res. Lett.*, 42, 4716-4722, doi:10.1002/2015GL064294.

Sandholt, P. E., and C. J. Farrugia, Monitoring magnetosheath-magnetosphere interconnection topography from the aurora, *Ann. Geophys.*, 20, 629, 2002.

Shay, M. A., J. F. Drake, M. Swisdak, W. Dorland, and B. N. Rogers (2003), Inherently three-dimensional magnetic reconnection: A mechanism for bursty bulk flows?, *Geophys. Res. Lett.*, 30(6), 1345, doi:10.1029/2002GL016267.

Shepherd, L. S., and P. A. Cassak (2012), Guide field dependence of 3-D X-line spreading during collisionless magnetic reconnection, *J. Geophys. Res.*, 117, A10101, doi:10.1029/2012JA017867.

Sibeck, D. G., and N. Omidi (2012), Flux transfer events: Motion and signatures, *J. Atmos. Sol. Terr. Phys.*, 87-88, doi:10.1016/j.jastp.2011.07.010.

Swisdak, M., and J. F. Drake (2007), Orientation of the reconnection X-line, *Geophys. Res. Lett.*, 34, L11106, doi:10.1029/2007GL029815.

Tóth, G., I. V. Sokolov, T. I. Gombosi, D. R. Chesney, C. R. Clauer, D. L. De Zeeuw, K. C. Hansen, K. J. Kane, W. B. Manchester, R. C. Oehmke, K. G. Powell, A. J. Ridley, I. I. Roussev, Q. F. Stout, O. Volberg, R. A. Wolf, S. Sazykin, A. Chan, and B. Yu (2005), Space Weather Modeling Framework: A new tool for the space science community, *J. Geophys. Res.*, 110, A12226, doi:10.1029/2005JA011126.

Tóth, G., B. van der Holst, I.V. Sokolov, D.L. De Zeeuw, T.I. Gombosi, F. Fang, W.B. Manchester, X. Meng, D. Najib, K G. Powell, Q. F. Stout, A. Gloer, Y.-J. Ma, M. Opher (2012), Adaptive Numerical Algorithms in Space Weather Modeling, *J. Computational Phys.*, 231, 870-903.

Trenchi, L., M. F. Marcucci, G. Palocchia, G. Consolini, M. B. Bavassano Cattaneo, A. M. Di Lellis, H. Reme, L. Kistler, C. M. Carr, and J. B. Cao (2008), Occurrence of reconnection jets at the dayside magnetopause: Double Star observations, *J. Geophys. Res.*, 113, A07S10, doi:10.1029/2007JA012774.

Tripathi, D., Isobe, H., and Mason, H. E. (2006), On the propagation of brightening after filament/prominence eruptions, as seen by SoHO-EIT, *A&A*, 453, 1111, doi:2006A&A453.1111T.

Walsh, B. M., C. M. Komar, and Y. Pfau-Kempf (2017), Spacecraft measurements constraining the spatial extent of a magnetopause reconnection X line, *Geophys. Res. Lett.*, 44, doi:10.1002/2017GL073379.

- 339 Walsh, B. M., D. G. Sibeck, Y. Wang, and D. H. Fairfield (2012), Dawn-dusk  
340 asymmetries in the Earth's magnetosheath, *J. Geophys. Res.*, *117*, A12211,  
341 doi:10.1029/2012JA018240.
- 342 Welling, D. T., and M. W. Liemohn (2014), Outflow in global magnetohydrodynamics as  
343 a function of a passive inner boundary source, *Journal of Geophysical Research: Space*  
344 *Physics*, *119*, pp. 2691-2705, doi:10.1002/2013JA019374.
- 345 Zou, Y., Walsh, B. M., Nishimura, Y., Angelopoulos, V., Ruohoniemi, J. M., McWilliams,  
346 K. A., and Nishitani, N. (2018), Spreading speed of magnetopause reconnection X-lines  
347 using ground-satellite coordination. *Geophys. Res. Lett.*, *45*. doi:10.1002/2017GL075765.

Figure 1.

Author Manuscript

Initial Patch



Extended Reconnection

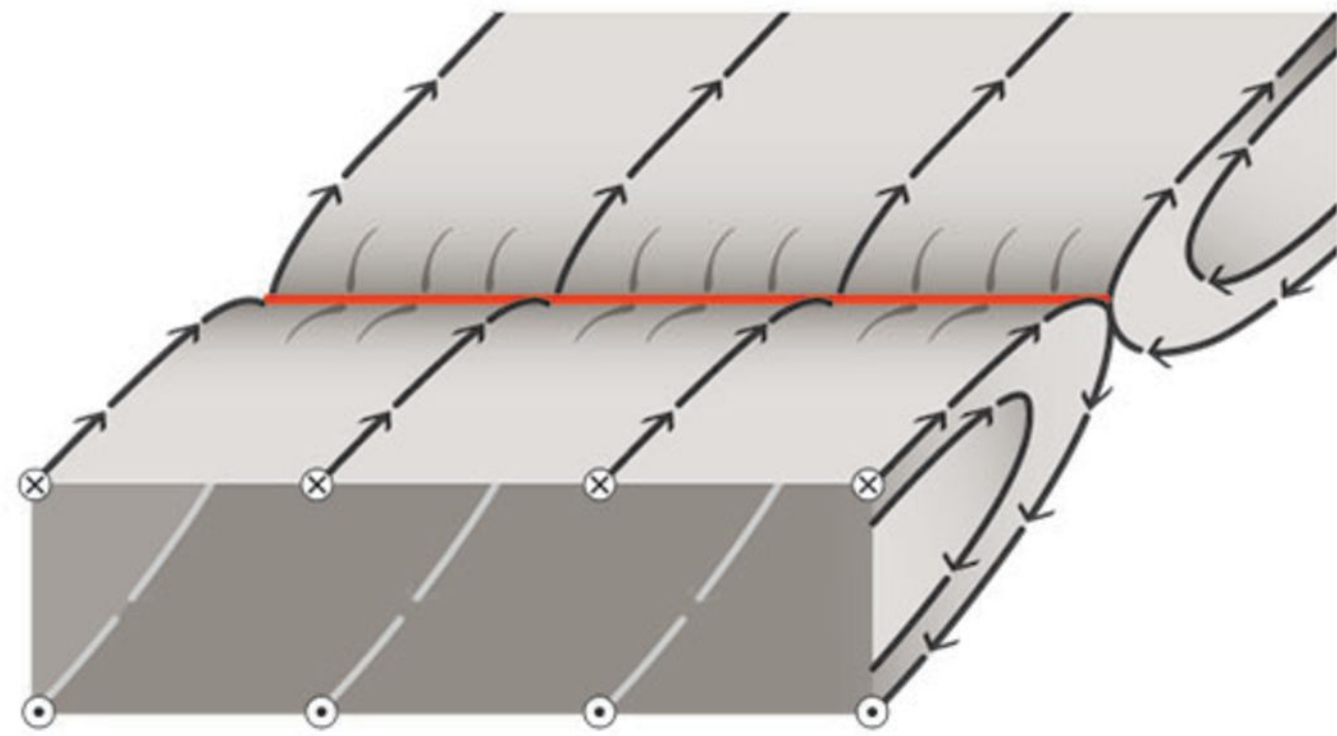
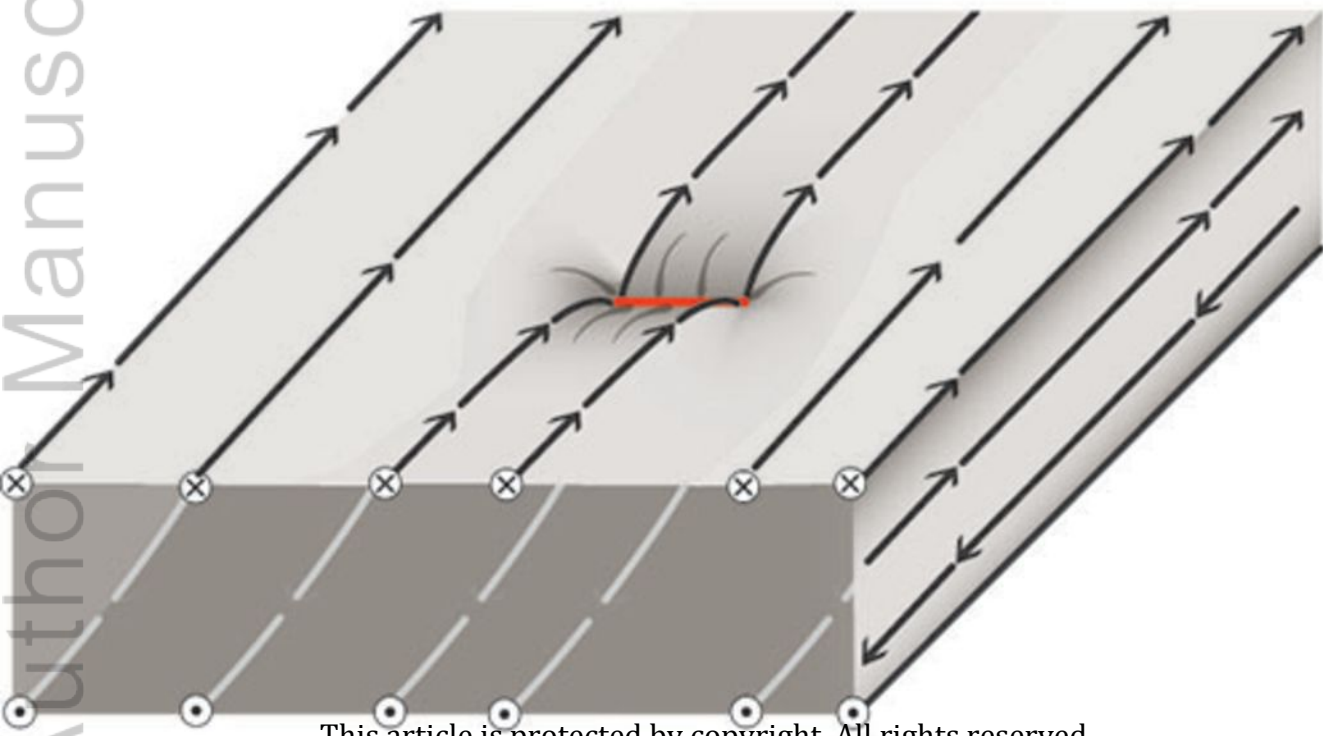


Figure 2.

Author Manuscript

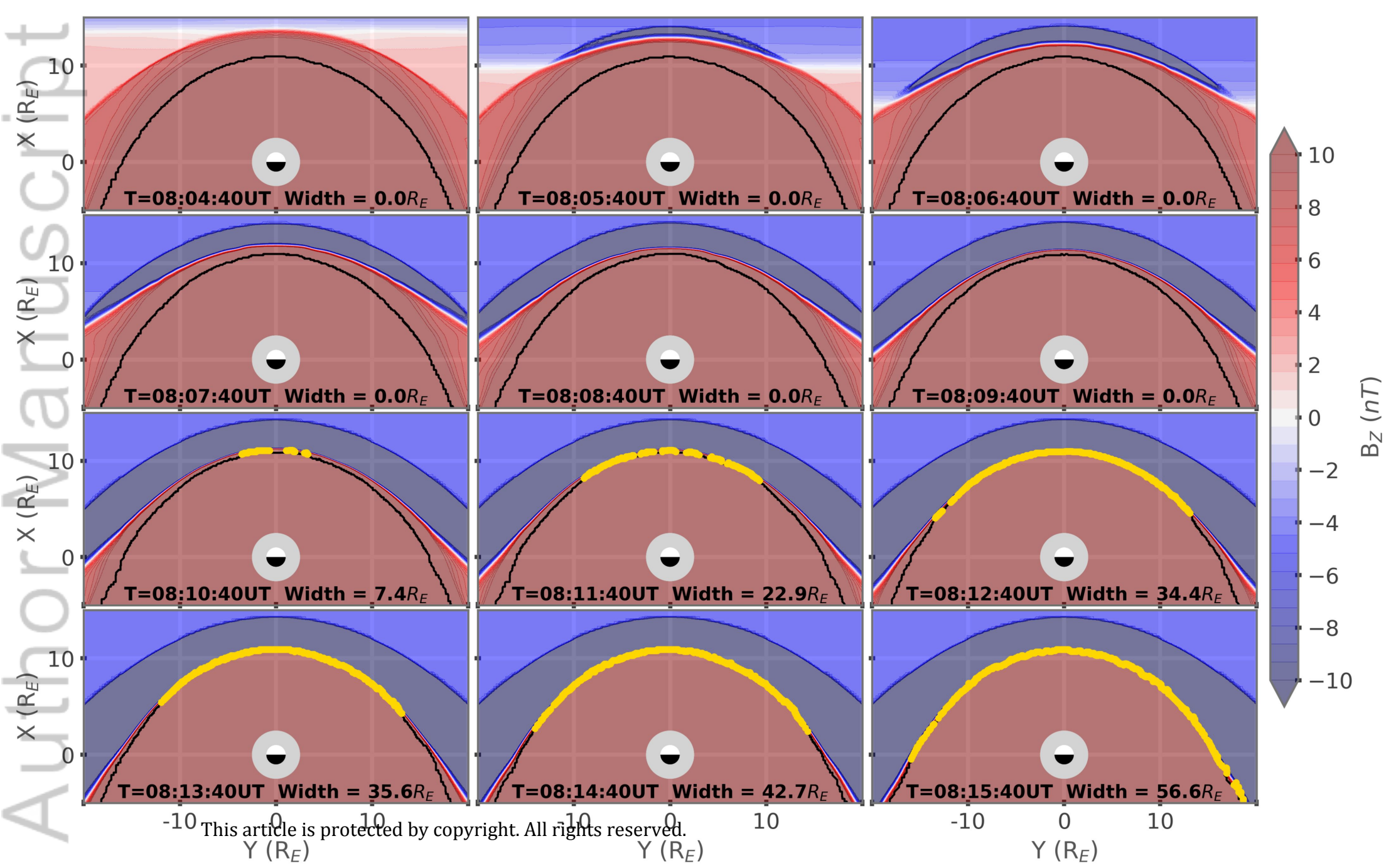


Figure 3.

Author Manuscript

# Reconnection Region Conditions

